TiO₂-based Transparent Conducting Oxide

Taro Hitosugi

Advanced Institute for Materials Research (WPI-AIMR)
Tohoku University

We review the properties of TiO$_2$-based transparent conducting oxide (TCO), which exhibit transparent conducting properties comparable to those of In$_{2-x}$Sn$_x$O$_3$ (ITO), the most widely used TCO. Epitaxial thin films of anatase Ti$_{1-x}$Nb$_x$O$_2$ (TNO) with 0.03 $\leq x \leq$ 0.06 exhibited a resistivity (ρ) of 2-3×10^{-4} Ωcm and internal transmittance of ~95% in the visible light region. Furthermore, polycrystalline films deposited on glass by the pulsed laser deposition and sputtering methods showed a ρ of 4.6×10^{-4} and 6.4×10^{-4} Ωcm, respectively, at room temperature. We also highlight those characteristics that are unique to TNO, which distinguish it from ITO, such as high refractive index, high transmittance in infrared, and high stability in reducing atmospheres. Possible applications of TNO, as well as the mechanism of transparent conducting properties found in this *d*-electron based TCO, are discussed. (Feb. 9, 2008)

1. Introduction

The development of transparent conducting oxides (TCOs) has led to the evolution of a variety of optoelectronic devices, such as flat panel displays (FPDs), touch panels, and Si-based solar cells (Fig. 1).[1,2] In newly emerging devices, including organic light-emitting diodes (LEDs), copper indium gallium diselenide (CIGS) solar cells, and blue GaN-based LEDs, TCOs have been key materials. Currently, In$_{2-x}$Sn$_x$O$_3$ (ITO) is the most widely used TCO because of its excellent transparent conducting properties[3,4] and its ease of fabrication.

However, there is still a strong demand for new TCOs, for two main reasons. One is the industrial need for high-efficiency optoelectronic de-

vices. The properties of TCO greatly improve device performance. For example, the use of a TCO whose refractive index matches that of GaN would significantly increase the external quantum efficiency of blue LEDs.[5] Furthermore, the appro-

priate TCOs with a high transmittance in the infrared region and a suitable work function would improve the efficiency of solar cells[6] and organic LEDs, respectively.

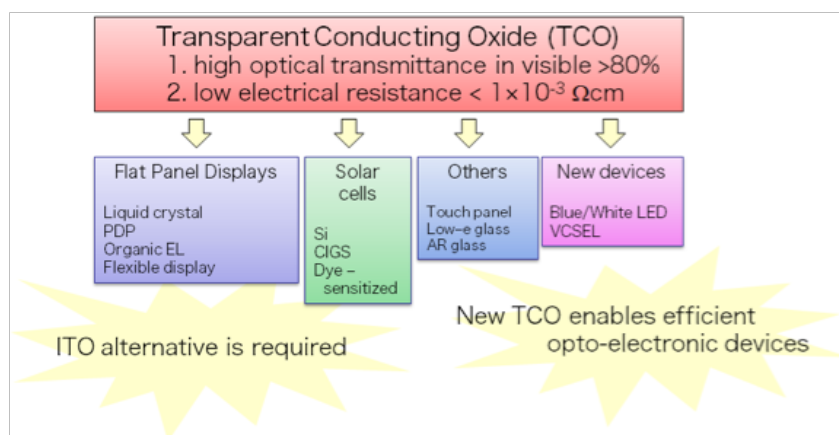The second reason concerns a resource problem: the

Figure 1 Widespread usage of transparent conducting oxides (TCO).

supply of indium (In), categorized as a rare metal, is unstable despite its rapidly expanding consumption, triggered by commercialization of wide-area FPDs. This has been stimulating research into new TCO materials composed of more abundant elements, as well as efforts toward the reduction of In use and recycling of In. Although ZnO, SnO_2 and many kinds of multi-component materials are promising alternatives to ITO,[7] it is still necessary to explore new TCO materials to widen the application fields of TCOs.

In this article, we review the properties of a new TCO, anatase $Ti_{1-x}Nb_xO_2$ (TNO),[8,9] which possesses electrical and optical properties comparable to those of ITO. Anatase TiO_2 is suitable as a mother compound of TCO: it is characterized by a wide band gap (3.2 eV)[10] and a relatively low effective mass of ~1 m_0 (m_0: free electron mass).[11] In addition, TNO has properties that ITO does not possess, such as, high refractive index, high transmittance in the infrared region, and high chemical stability in reducing atmosphere. We expect that these properties will allow the use of TNO in fabricating new, high-efficiency optoelectrical devices. Moreover, Ti, a major constituent of TNO, is much more abundant in the earth's crust than indium, by a factor of roughly 10^5.[12]

This article is organized as follows. In the next section, we briefly introduce the basic electronic properties and film growth of TiO_2. The semiconductor-to-metal transition that occurs upon doping TiO_2 with Nb is described in Section 3. Section 4 presents an application-oriented topic: deposition of polycrystalline TiO_2-based transparent conductors on glass substrate. In Section 5, we discuss the carrier transport in TNO, explaining the difference between TNO and conventional TCOs with regard to the mechanism giving rise to transparent conductivity. In Section 6, we discuss the future prospects of this material.

2. Titanium Dioxide (TiO_2)

Titanium dioxide (TiO_2) has been studied intensively over the last decade because of its usefulness in a wide variety of applications, including catalysis,[13] pigments, and sensors.[14] More recently, TiO_2 has attracted much attention as an electronic material, and attempts at employing it as a high-k material[15] and in resistive random access memory (RRAM)[16] devices have been made. Diluted magnetic semiconductors based on TiO_2 have the potential to enable room-temperature spintronics.[17] Reviews on properties of TiO_2 in relation to its applications can be found elsewhere.[18,19]

Among the many polytypes of TiO_2, the technologically important crystal structures are rutile and anatase (Fig. 2 and Table 1). The rutile phase has been studied extensively as a typical transition metal oxide. Its electronic structure, transport and
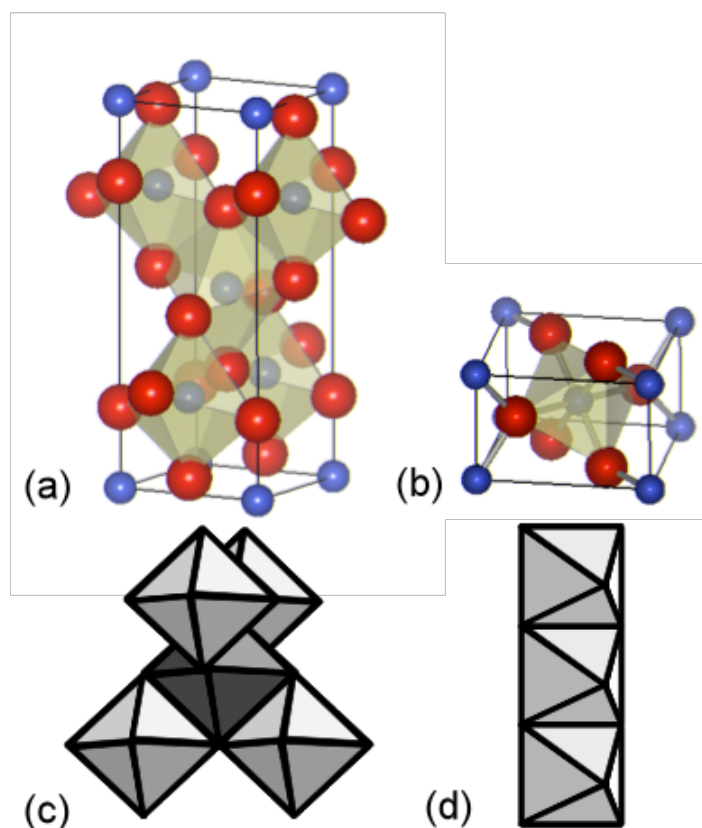

Figure 2 Crystal structures of (a) anatase and (b) rutile, and a schematic of the TiO_6 networks in (c) anatase and (b) rutile. Red and blue spheres denote Ti and O atoms, respectively.

		rutile	anatase
lattice parameter	a	0.4584	0.3733
	b	-	-
	c	0.2953	0.937
density (Kg/m³)		4240	3830

Table 1 Structural and electrical parameters of rutile and anatase. Lattice parameter and density are adopted from ref. 14.

optical properties, and surface structure have been thoroughly reported. Both rutile and anatase, with their tetragonal symmetry, can be described as a network of TiO_6 octahedra. The two structures differ in the distortion and linkage of the octahedra. In the anatase structure, each octahedron is in contact with eight neighbors (four sharing edges and four sharing corners), as shown in Fig. 2(c), while the coordination number of rutile is 10 (two sharing edges and eight sharing corners) (Fig. 2(d)).

Anatase TiO_2 tends to be oxygen-deficient, which can be expressed as $TiO_{2-\delta}$. The degree of oxygen deficiency δ can be con-trolled by adjusting the conditions of film growth and/or post-deposition annealing. The oxygen vacancies generate n-type carriers in the Ti-3d conduction band. Thus, the resistivity (ρ) of TiO_2 can be controlled by δ. Oxygen-deficient $TiO_{2-\delta}$ films, however, lose transparency, so that they cannot be used as a TCO. In addition to the introduction of oxygen deficiencies, the substitution of Nb for Ti could provide carriers. Indeed, it is known that Nb-doping of rutile TiO_2 decreases ρ by a factor of more than 5500,[20] although the minimum ρ value ($\sim 10^{-2}$ Ωcm at room temperature)[21,22] is not sufficient for TCO

applications because of low electron mass (< 1 m_0) in rutile.[23]

It is believed that anatase, which has a higher mobility than rutile, is more suited to TCO. However, transport properties of anatase have not been well studied, since bulk anatase is difficult to grow because it is thermodynamically not a stable structure. Lévy *et al.* were the first to report single-crystal growth of anatase using chemical vapor transport.[24] They measured the optical and transport properties, and obtained a ρ of $\sim 10^{-1}$ Ωcm with an electron mobility exceeding 600 cm²/Vs at 50 K.[25] Nb-doping of bulk anatase has been investigated by Mulmi *et al.*, who reported ρ values of $\sim 5 \times 10^{-2}$ Ωcm.[26] Their ρ vs. temperature (ρ-T) curve showed a semiconducting behavior, possibly due to the rather low dopant (Nb) concentration.

TiO_2 films have been fabricated by various techniques.[27,28] These include sputtering, pulsed laser deposition, molecular beam epitaxy, chemical vapor deposition, sol-gel, and spray pyrolysis. Also, epitaxial thin films with different orientations have been de-

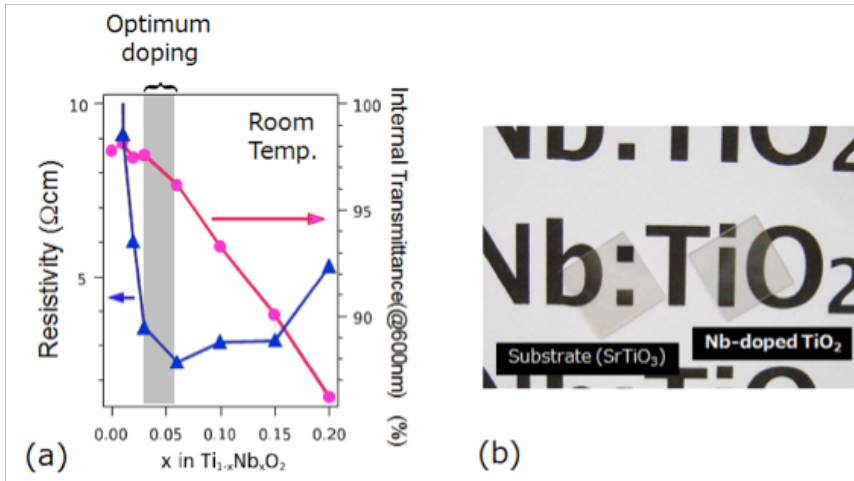| Crystal structure	Out of plane orientation	Substrate
anatase	(001)	$SrTiO_3(100)$, $LaAlO_3(100)$, $LaSrAlO_4(100)$, $LSAT((LaAlO_3)_{0.3}(Sr_2AlTaO_6)_{0.7})$ (100), $NdGaO_3(110)(001)$
anatase	(102)	$SrTiO_3(110)$ $LaAlO_3(110)$, $NdGaO_3(100)$
anatase	(112)	$Al_2O_3(0001)$
rutile	(100)	$Al_2O_3(0001)$, $GaN(0001)$, $ZnO(0001)$
rutile	(101)	$Al_2O_3(10\text{-}12)$ r-surface
rutile	(001)	$Al_2O_3(10\text{-}10)$ m surface

Table 2 Substrates for epitaxial growth

Figure 3 (a) Resistivity and internal transmittance (@ 600 nm) of Ti$_{1-x}$Nb$_x$O$_2$. (b) Photograph of SrTiO$_3$ substrate and Ti$_{0.94}$Nb$_{0.04}$O$_2$ epitaxial thin film on SrTiO$_3$(100).

posited by choosing appropriate substrates, as summarized in Table 2.

3. Nonmetal – metal transition & Transparent conducting properties

A dramatic nonmetal-metal transition takes place on doping anatase with Nb. Figure 3(a) plots the ρ values of Ti$_{1-x}$Nb$_x$O$_2$ epitaxial thin films against x. These epitaxial thin films were grown by using the pulsed laser deposition (PLD) technique on SrTiO$_3$(100) or LaAlO$_3$(100) substrates.[8,9] X-ray diffraction (XRD) measurements confirmed that the anatase was single-phase and free of any impurities. Undoped anatase TiO$_2$ exhibited a ρ on the order of 10^{-1} Ωcm. Nb doping caused a marked decrease in ρ, by a factor of 10^3. The minimum ρ value (2×10^{-4} Ωcm at 300 K) was obtained at $x = 0.06$, where a metallic temperature dependence (dρ/d$T > 0$) was observed.

Figure 3(a) also shows the internal optical transmittance at 600 nm, as evaluated from the extinction coefficient. The trans-

mittance gradually decreases with Nb doping, mainly due to the light absorption of charge carriers. As seen from Fig. 3, both high electrical conductivity and high optical transmittance can be achieved for $0.03 \leq x \leq 0.06$. It should be emphasized that the ρ values in this optimal range are as low as 2-3×10^{-4} Ωcm, which is comparable to those of conventional ITO films.[3] Fig. 3(b) shows pictures of a SrTiO$_3$ substrate and Nb-doped TiO$_2$ (TNO) film grown on SrTiO$_3$, demonstrating the high optical transparency of TNO.
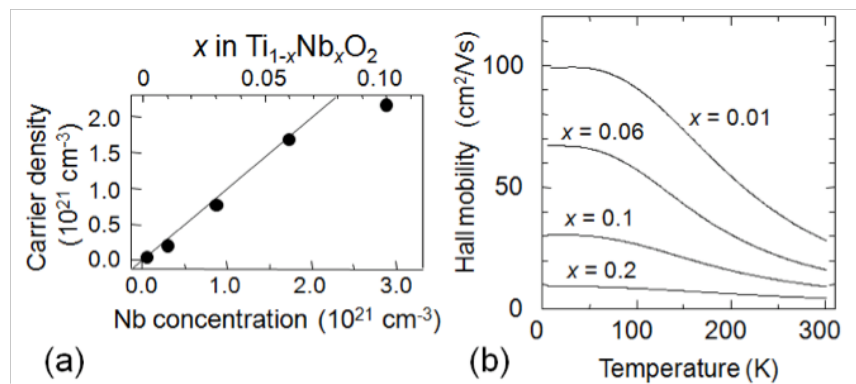
These highly conductive TNO films are in the degenerate semiconductor regime: The Nb dopant atoms occur as Nb^{5+} ions and release conduction electrons with high efficiency. Figure 4(a) plots carrier density, n_e, against x. There is a fairly linear relation between n_e and x up to an x value of ~0.06, which can be expressed as $n_e \approx 0.9 n_{Nb}$, where n_{Nb} is the density of Nb. This implies that Nb ions release conduction electrons with an efficiency of ~90%, up to $x = 0.06$. At higher doping levels ($x > 0.06$), the ionization efficiency is slightly suppressed. The Hall mobility, μ_H, increases as temperature (T) is lowered (Fig. 4(b)), which indicates that the room-temperature ρ values of TNO are dominated by phonon scattering. The films within the optimal x region ($0.03 \leq x \leq 0.06$) show μ_H (300 K) values of around 20 cm^{2}V^{-1}s^{-1}, which is approximately half that of ITO with the same ρ.[29]

After the first report on PLD growth of Ti$_{0.94}$Nb$_{0.06}$O$_2$ films by Furubayashi *et al.*, several groups have studied the deposition of TNO epitaxial thin films using PLD[30,31] and sputtering,[32,33] and obtained highly transparent con-

Figure 4 (a) Carrier density at 300 K as a function of Nb concentration and x. (b) Hall mobility as a function of temperature.

ducting properties. Anatase films doped with Ta show similar electric properties.[34] In contrast, W-doped anatase, in which each dopant ion (W^{6+}) is expected to release two electrons, is less conductive than Nb- and Ta-doped anatase.[35]

4. Polycrystalline films on glass substrate

From a practical viewpoint, TCO films need to be coated on glass and plastics. Considerable efforts have been devoted to the deposition of TCO films on glass in particular because of the increasing technological demands for flat panel displays and solar cells. Very recently, we have attempted to grow TNO films on glass by PLD, and obtained $\rho = 4.6 \times 10^{-3}$ Ωcm,[36] which satisfies the practical requirement for TCOs: $\rho < 10^{-4}$ Ωcm.

These films were prepared on glass by crystallizing from an amorphous phase (Fig. 5(a)). The crystallization process is accompanied by a 10^6-fold drop in ρ (Fig. 5(b)). Furthermore, we have applied this technique to TNO films that were sputter-deposited on glass substrates, and obtained a ρ of 6.4×10^{-4} Ωcm at room temperature, with an absorption of less than 10% in the visible region.[10] Shigesato et al. recently reproduced this film preparation process by using the DC sputtering method.[11]

The recipe for fabricating TNO films using sputtering is as follows. 1) Amorphous $Ti_{0.94}Nb_{0.06}O_2$ films are deposited using a commercial sputtering apparatus on unheated non-alkali glass (Corning 1737) substrates (Fig. 6(a)). A sintered pellet with a
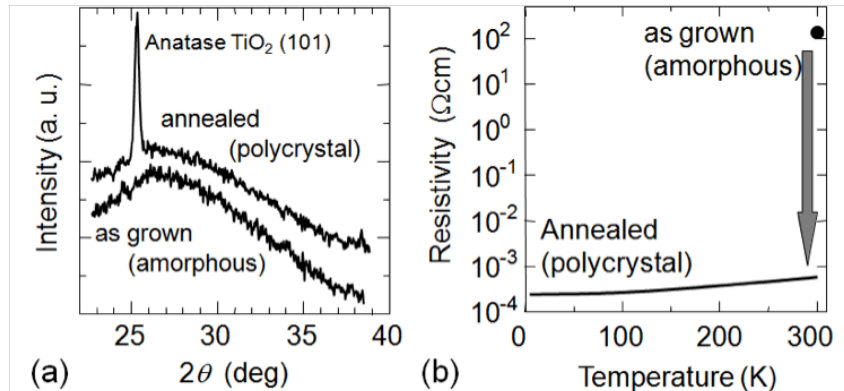

Figure 5 (a) X-ray diffraction patterns of the $Ti_{0.94}Nb_{0.06}O_2$ film before (as-grown, amorphous) and after H_2 annealing at 500ºC. Amorphous film crystallizes upon annealing. (b) Resistivity of as-grown amorphous film and annealed film. The annealed film shows a positive temperature coefficient indicative of metallic behavior.

nominal composition of $Ti_{0.94}Nb_{0.06}O_{2-\delta}$ or Ti metal is used as a sputtering target, and the deposition time is adjusted so as to obtain films with thicknesses of ~200 nm. 2) The as-grown films are then annealed in vacuum using a rapid thermal annealing furnace, in which the annealing temperature is raised to 500°C
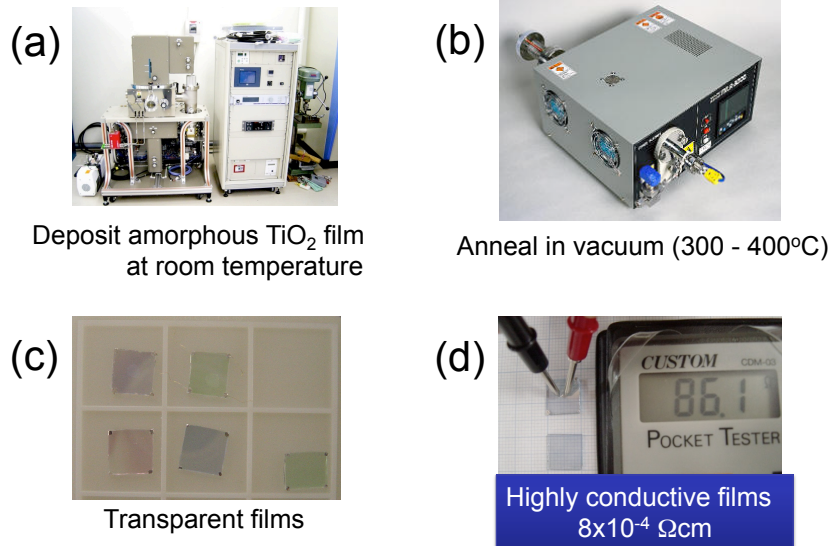

Figure 6 Preparation process of TiO_2-based TCO on glass substrate. (a) Deposition of an amorphous TiO_2 film at room temperature by the sputtering technique. (b) Annealing of the amorphous film in vacuum at 300 – 400ºC. Annealing for 5 minutes is enough to obtain highly conductive films. (c) Photographs of films on glass. The films appear colored due to the interference effect. (d) Demonstration of excellent conductivity of TiO_2-based TCO films.

within 5 min (Fig. 6(b)). Annealing for 5 min is enough to obtain highly conducting films. The annealing furnace is evacuated to 10^{-4} Torr, in order to remove residual oxygen from the furnace. Images of typical films are shown in Figs. 6(c) and (d). Note that the films are colored due to optical interference.

The most important factor for obtaining high-conductivity TNO films is to control the oxygen stoichiometry in the films. We start with an oxygen-deficient $Ti_{0.94}Nb_{0.06}O_{2-\delta}$ target with shiny black color. It is also possible to use Nb-doped TiO or Ti_2O_3 as a sputtering target.[39] The oxygen partial pressure during deposition should be maintained at around 1×10^{-3} Pa in order to have precise control over the oxygen content of the films. Annealing conditions have a great influence on the electrical properties of TNO. Annealing in air at 600°C yields insulating films with $\rho > 10^6$ Ωcm.

The minimum ρ achieved by this annealing process using sputtering-based-approach is 8×10^{-4} Ωcm, which is very low for a transition metal oxide in polycrystalline form.[40] By introducing a seed layer, we could obtain films having a ρ of 6.4×10^{-4} Ωcm. The seed layer acts as a template for anatase growth, and also serves as a crystal growth center, resulting in a decrease in crystallization temperature. Table 3 summarizes the growth conditions and the ρ values obtained. Detailed deposition parameters have been reported elsewhere.[41,42] Very recently, we have succeeded in preparing conductive films by annealing amorphous films in air at 300-400°C.[43]

Polycrystalline TNO films with ρ values on the order of 10^{-4} Ωcm

Composition $Ti_{1-x}Nb_xO_2$ (Target) (Film)	Substrate	$f(O_2)$ (Top layer) (Seed layer)	Annealing Condition (Temperature) (Atmosphere)	Resistivity
$x = 0.06$ -	non-alkaline glass	0.05% 5%	400°C Vacuum	6.4×10^{-4} Ωcm
$x = 0.06$ -	non-alkaline glass	0.05% No seed layer	400°C Vacuum	7.6×10^{-4} Ωcm
$x = 0.037$ -	polyimide	0.05% 5%	300°C H_2	1.9×10^{-3} Ωcm

Table 3. Growth and annealing conditions and resistivity values obtained for polycrystalline Nb-doped anatase TiO_2 thin films.

exhibit a metallic ρ - T behavior. This suggests that the carrier transport is less affected by grain boundaries. Furthermore, the n_e value is as high as ~1.6×10^{21} cm^{-3}, from which the ionization efficiency is estimated to be ~90%. These results lead us to conclude that the dopant Nb is substituted for the Ti site in anatase without segregation even in polycrystalline films. Uniquely, TNO has a higher activation efficiency in

(a)

(b)

Figure 7 (a) Transmittance, reflectance, and (b) absorbance spectra of a typical anatase $Ti_{0.94}Nb_{0.06}O_2$ film on glass substrate.

both epitaxial and polycrystalline films compared with other conventional TCOs (typically < 50% in the case of ITO).[44,45,46]

Transmittance (T_r) and reflectance (R) spectra of a TNO film after annealing (thickness $\approx$ 200 nm) are shown in Fig. 7(a). The T_r value throughout the wavelength range of 400-1500 nm is 60-80%, which is lower than those of typical ITO films. This is due to the relatively high refractive index of anatase TNO (~2.4 at 500 nm), which tends to enhance R and thus suppress T_r. The absorbance (A) in the visible region, calculated from the equation $A = 1-(T_r+R)$, is below 10% (Fig. 7(b)).
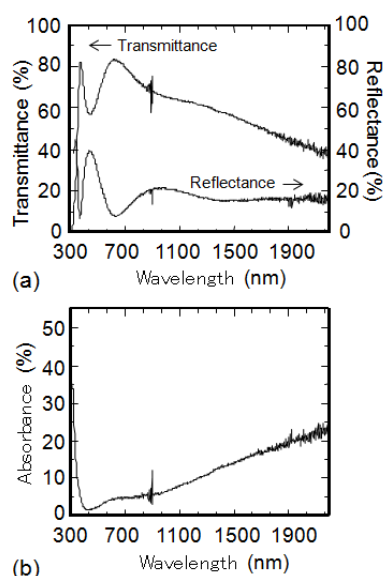
5. Mechanism of transparent conductivity

In order to understand the mechanism of transparent conductivity in TNO, we performed a first-principles band calculation with generalized gradient approximation (GGA)[47] and resonant photoemission measurements.[48]

Figure 8(a) shows density of states (DOS) as a function of electron energy calculated for undoped anatase TiO_2. The figure exhibits a band gap of about 2.24
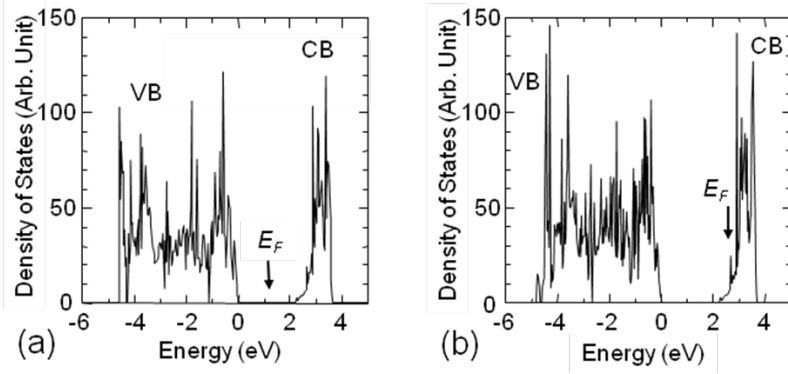
Figure 8 Density of states calculated for (a) undoped and (b) Nb-doped anatase. The origin of energy (E = 0) corresponds to the top of the valence band (VB). Note that the Fermi energy (E_F) shifted into the conduction band (CB) upon Nb doping.

eV, which is somewhat smaller than the empirical value of 3.2 eV. This underestimation of the band gap is a well-known limitation of GGA calculations. The Fermi energy (E_F) lies in the middle of the band gap, reflecting the insulating behavior of pure anatase TiO_2.

Figure 8(b) is a total DOS profile calculated for $Ti_{1-x}Nb_xO_2$. In the calculation, the central Ti atom in a supercell is substituted for Nb, corresponding to a doping content x of ~0.0625. Notably, the Fermi energy (E_F) is located inside the conduction band, implying that $Ti_{1-x}Nb_xO_2$ can be described as a normal metal. This is consistent with experimentally observed positive $d\rho/dT$ and temperature-independent n_e.[8] Another interesting feature seen in Fig. 8(b) is that no impurity state exists in the in-gap region, which explains the high optical transparency in the visible region.

Partial DOS profiles of Ti 3d and Nb 4d states above E_F have essentially identical shapes (not shown in figure). That is, the Nb 4d orbital spreads over the entire region of the conduction band, suggesting that Nb is strongly hy-

bridized with Ti. As a result of the strong Ti-Nb hybridization, each Nb atom releases one electron to the conduction band, leading to a high n_e (>10^{21} cm^{-3}). Interestingly, hybridization is a unique feature of the anatase structure. Nb-doped rutile TiO_2 shows semiconducting carrier transport with $d\rho/dT < 0$ as a result of the formation of shallow Nb impurity states.[49]

A finite DOS at E_F was clearly observed by Ti 2p-3d resonant photoemission spectroscopy,
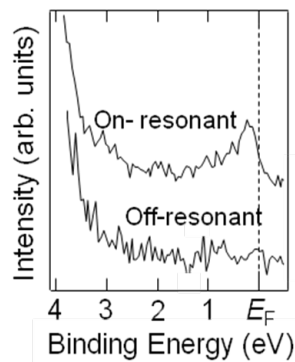

Figure 9 Off-resonant (hν = 600 eV) and Ti 2p-3d resonant (hν = 461.2 eV) X-ray photoemission spectra of anatase $Ti_{0.94}Nb_{0.06}O_2$.

which intensifies the states contributed by the Ti orbital. Figure 9 shows off-resonant (hν = 600 eV) and Ti 2p-3d resonant (hν = 461.2 eV) spectra of $Ti_{0.94}Nb_{0.06}O_2$ near the band gap. The on-resonant spectrum exhibits a clear peak at E_F, corresponding to the bottom of the Ti 3d conduction band, whereas the spectral weight observed in the off-resonant spectra near E_F is negligible small. This proves that conduction electrons indeed have a d-electron nature, as predicted by the band calculations. Moreover, we could not detect any impurity states inside the band gap, which is consistent with the GGA calculation described above.

So far, we have discussed the carrier introduction mechanisms of TNO in terms of high ionization efficiency. From the viewpoint of optical transmittance, however, a large n_e due to high ionization efficiency is not favorable because carriers absorb light and thus degrade optical transparency. The compromise between conductivity and transparency is always a crucial issue for TCOs.

The most important optical parameter of TCO is transparency at 400-800 nm (visible region). At wavelengths shorter than 400 nm, a strong absorption occurs due to the fundamental band gap. At longer wavelengths in the infrared region, absorption also occurs due to the interaction between free electrons and electromagnetic waves. In the infrared region, transmission characteristics of light is determined by the plasma wavelength, λ_p,[50]

$$\lambda_p = 2\pi c \left(\frac{\varepsilon_0 \varepsilon_\infty m^*}{n_e e^2} \right)^{\frac{1}{2}} \quad (1),$$

where ε_0, ε_∞, c, m^*, n_e, and e denote the dielectric constant of

$$\lambda_p \propto \left(\frac{\varepsilon_0 \varepsilon_\infty m_c^*}{ne^2} \right)^{\frac{1}{2}}$$

Plasma wavelength

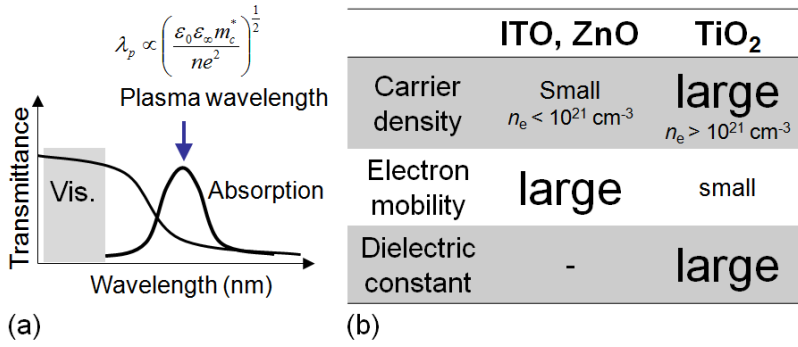|	ITO, ZnO	TiO₂
Carrier density	Small $n_e < 10^{21}$ cm⁻³	large $n_e > 10^{21}$ cm⁻³
Electron mobility	large	small
Dielectric constant	-	large

(a)   (b)

Figure 10 (a) Transmittance and absorption spectra of a transparent conductor. The plasma wavelength must be greater than 800 nm in order to ensure transparency in the visible range. (b) Comparison of material parameters between conventional TCOs (ITO, ZnO, SnO₂, etc.) and the TiO₂-based TCO.

vacuum, the high-frequency permittivity, the speed of light, the conductivity effective mass, and the electronic charge, respectively. At λ_p, free electrons resonate with the alternating electric field and the absorbance shows a maximum, and electromagnetic waves with wavelengths shorter than λ_p can pass through a film. Consequently, λ_p needs to be much larger than 800 nm in order to ensure sufficient transparency in the visible region, as shown in Fig. 10(a).

As n_e is increased, λ_p decreases, and, thus, the absorption of visible light becomes significant. In conventional TCOs, n_e is adjusted to be less than 1×10^{21} cm⁻³, and this relatively low n_e is compensated by high electron mobility (Fig. 10(b)). By contrast, in the case of TNO films, n_e could easily exceed 10^{21} cm⁻³, retaining excellent transparency. This can be explained by the relatively large dielectric constant of TiO₂. That is, as can be seen from Eq. (1), larger dielectric constants increase the λ_p, and, thus, recover transparency in the visible light region.

It should be stressed that the transmittance of TNO in the infrared region is higher than that of ITO with the same n_e. This is of great advantage in certain applications, such as solar cells, in which high transmittance in the infrared is highly desired.[51]

A large dielectric constant is thought to have a strong effect on the transport properties of TNO: Owing to the large ε, electronic charges associated with impurities are effectively screened (Thomas-Fermi screening), resulting in a substantial suppression of carrier scattering by impurities. This explains how TNO maintains a high mobility even when it is heavily doped with Nb.

6. Prospects for applications

It is of crucial importance to find applications for TiO₂-based TCOs, exploiting their unique characteristics. As mentioned earlier, TNO has remarkable properties that ITO does not have, such as high refractive index (~2.4 at a wavelength of 500 nm), high transmittance in the infrared region, and high stability in reducing atmosphere. Development of optoelectronic devices on the basis of such properties would expand the use of TCOs and generate a new market. Electrodes of blue LEDs and solar cells are among the promising potential applications of TNO. Furthermore, TNO is a d-electron based TCO system (Fig. 11), in sharp contrast to conventional TCOs, which are based on s electrons. Combining TCO properties with a d-electron nature might lead to new spintronic devices.

A lower ρ and higher transmittance are still required for
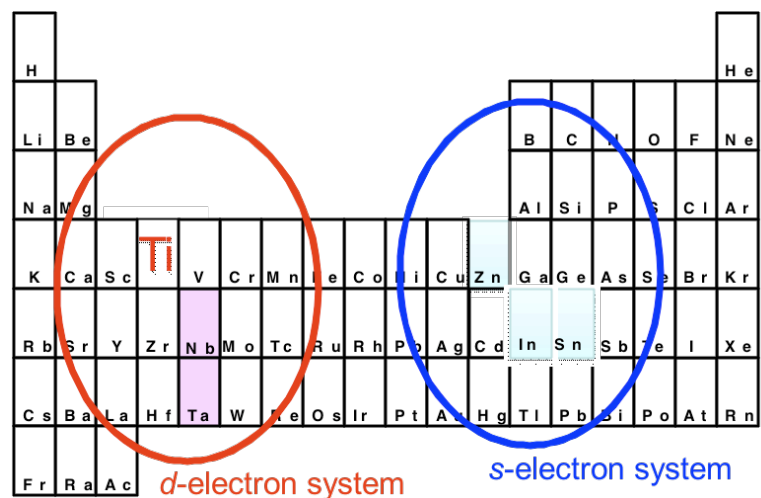
Figure 11 Anatase Ti$_{1-x}$Nb$_x$O₂ as a d-electron-based TCO.

TNO. A deeper understanding of carrier transport in TNO polycrystalline films and the exploration of dopants other than Nb, with the aid of theoretical predictions, remain challenging issues, which would pave the way towards post-ITO materials.

CONCLUSIONS

We reported the development of anatase TiO_2-based transparent conducting oxides (TCOs). Epitaxial films of Nb-doped TiO_2 (TNO) exhibit a low ρ of $\sim 2\times10^{-4}$ Ωcm and high optical transmittance in the visible region. We also succeeded in preparing highly conductive TNO polycrystalline films on glass substrates by the sputtering technique. The polycrystalline films showed excellent transparency with an absorption of less than 10%. These encouraging results suggest that it might soon be possible to use wide-area polycrystalline TNO films as transparent electrodes. We have also demonstrated that TNO is a promising alternative to ITO. Given that TNO is a d-electron-based TCO, it is expected that the present results will stimulate material exploration into new d-electron-based TCOs.

References

[1] D. S. Ginley and C. Bright, Mater. Res. Bull. 25, 15 (2000).

[2] H. L. Hartnagel, A. L. Dawar, A. K. Jain, and C. Jagadish, Semiconducting Transparent Thin Films; Institute of Physics: Bristol, UK, 1995.

[3] C. A. Pan and T. P. Ma, Appl. Phys. Lett. 37, 163 (1980).

[4] I. Hamberg and C. G. Granqvist, J. Appl. Phys. 60, R123 (1986).

[5] J.-H. Lim, D.-K. Hwang, H.-S. Kim, J.-Y. Oh, J.-H. Yang, R. Navamathavan, and S.-J. Park, Appl. Phys. Lett. 85, 6191 (2004).

[6] M. Kambe, K. Sato, D. Kobayashi, Y. Kurokawa, S. Miyajima, M. Fukawa, N. Taneda, A. Yamada, and M. Konagai, Jpn. J. Appl. Phys. 45, L291 (2006).

[7] T. Minami, Mater. Res. Bull. 25, 38 (2000).

[8] Y. Furubayashi, T. Hitosugi, Y. Yamamoto, K. Inaba, G. Kinoda, Y. Hirose, T. Shimada, and T. Hasegawa, Appl. Phys. Lett. 86, 252101 (2005).

[9] T. Hitosugi, Y. Furubayashi, A. Ueda, K. Itabashi, K. Inaba, Y. Hirose, G. Kinoda, Y. Yamamoto, T. Shimada, and T. Hasegawa, Jpn. J. Appl. Phys. 44, L1063 (2005).

[10] H. Tang, H. Berger, P. E. Schmid, F. Lévy, and G. Burri, Solid State Commun. 23, 161 (1977).

[11] H. Tang, K. Prasad, R. Sanjines, P. E. Schmid, and F. Lévy, J. Appl. Phys. 75, 2042 (1994).

[12] S. R. Taylor, and S. H. McLennan, The Continental Crust: Its Composition and Evolution, Blackwell, Oxford, p.312 (1985).

[13] A. Fujishima and K. Honda, Nature 37, 238 (1972).

[14] O. Carp, C. L. Huisman, and A. Reller, Prog. Solid State Chem. 32, 33 (2004).

[15] A. I. Kingon, J.-P. Maria, S. K. Streiffer, Nature 406, 1032 (2000).

[16] M. Fujimoto, H. Koyama, M. Konagai, Y. Hosoi, K. Ishihara, S. Ohnishi, and N. Awaya, Appl. Phys. Lett. 89,. 223509 (2006).

[17] Y. Matsumoto, M. Murakami, T. Shono, T. Hasegawa, T. Fukumura, M. Kawasaki, P. Ahmet, T. Chikyow, S. Koshihara, and H. Koinuma, Science 291, 534 (2001).

[18] K. Hashimoto, H. Irie, and A. Fujishima, Jpn. J. Appl. Phys. 44, 8269 (2005).

[19] T. Fukumura, H. Toyosaki and Y. Yamada, Semicond. Sci. Technol. 20, S103 (2005).

[20] F. A. Grant, Rev. Mod. Phys. 31, 646 (1959).

[21] Y. Furubayashi, T. Hitosugi, and T. Hasegawa, Appl. Phys. Lett. 88, 226103 (2006).

[22] S. X. Zhang, D. C. Kundaliya, W. Yu, S. Dhar, S.Y. Young, L. G. Salamanca-Riba, S. B. Ogale, R. D. Vispute, T. Venkatesan, Journal of Applied Physics 102, 013701 (2007).

[23] D. C. Cronemeyer, Phys. Rev. 87, 876 (1952).

[24] H. Berger, H. Tang, and F. Lévy, J. Cryst. Growth 130, 108 (1993).

[25] L. Forro, O. Chauvet, D. Emin, Z. Zuppiroli, H. Berger, F. Levy, J. Appl. Phys. 75, 633 (1994).

[26] D.D. Mulmi, T. Sekiya, N. Kamiya, S. Kurita, Y. Murakami, T. Kodaira, J. Phys. Chem. Sol. 65 1181 (2004).

[27] D. P. Norton, Mater. Sci. Eng. R 43 139 (2004).

[28] S.A. Chambers, Surf. Sci. Rep. 39, 105 (2000).

[29] Y. Shigesato, D. C. Paine, and T. E. Haynes, J. Appl. Phys. 73, 3805 (1993).

[30] D. Kurita, S. Ohta, K. Sugiura, H. Ohta, and K. Koumoto, J. Appl. Phys. 100, 096105 (2006).

[31] S. X. Zhang, S. Dhar, W. Yu, H. Xu, S. B. Ogale, and T. Venkatesan, Appl. Phys. Lett. 91 (2007) 112113.

[32] M. A. Gillispie, M. F. A. M. van Hest, M. S. Dabney, J. D. Perkins, D. S. Ginley, J. Appl. Phys. 101, 033125 (2007).

[33] M. S. Dabney, M. F. A. M. van Hest, C. W. Teplin, S. P. Arenkiel, J. D. Perkins, and D. S. Ginley, Thin Solid Films 516, 4133 (2008).

[34] T. Hitosugi, Y. Furubayashi, A. Ueda, K. Itabashi, K. Inaba, Y. Hirose, G. Kinoda, Y. Yamamoto, T. Shimada, and T. Hasegawa, Jpn. J. Appl. Phys. 44, L1063 (2005).

[35] Takeuchi *et al.*, in preparation.

[36] T. Hitosugi, A. Ueda, S. Nakao, Y. Furubayashi, N. Yamada, Y. Hirose, T. Shimada, and T. Hasegawa, Appl. Phys. Lett. 90, 212106 (2007).

[37] N. L. H. Hoang, N. Yamada, T. Hitosugi, J. Kasai, S. Nakao, T. Shimada, and T. Hasegawa, Appl. Phys. Express 1, 115001 (2008).

[38] Y. Sato, H. Akizuki, T. Kamiyama, and Y. Shigesato, Thin Solid Films 516, 5758 (2008).

[39] N. Yamada in preparation for publication.

[40] N. Tsuda, K. Nasu, A. Fujimori, K. Shiratori, Electronic Conduction in Oxides, Springer, Berlin, 2000.

[41] T. Hitosugi, N. Yamada, N. L. H. Hoang, J. Kasai, S. Nakao, T. Shimada, T. Hasegawa, Thin Solid Films, in press.
[42] N. Yamada, T. Hitosugi, N. L. H. Hoang, Y. Furubayashi, Y. Hirose, T. Shimada and T. Hasegawa, Jpn. J. Appl. Phys. 46, 5275-5277 (2007).

[43] S. Nakao *et al.*, in preparation.

[44] N. Yamada, I. Yasui, Y. Shigesato, H. Li, Y. Ujihira, and K. Nomura, Jpn. J. Appl. Phys. 39, 4158 (2000).

[45] H. Köstlin, R. Jost, and W. Lems, Phys. Stat. Sol(a) 29, 87 (1975).

[46] J. -C. Manifacier, L. Szepessy, J. F. Bresse, M. Perotin, R. Stuck, Mat. Res. Bull. 14, 163 (1079).

[47] H. Kamisaka, T. Hitosugi, T. Hasegawa, Suenaga, and K. Yamashita. submitted to Compu. Mater. Sci.

[48] T. Hitosugi, H. Kamisaka, K. Yamashita, H. Nogawa, Y. Furubayashi, S. Nakao, N. Yamada, N. Chikamatsu, H. Kumigashira, M. Oshima, Y. Hirose, T. Shimada, and T. Hasegawa, Appl. Phys. Express 1, 111203 (2008).

[49] D. Morris, Y. Dou, J. Rebane, C. E. J. Mitchell, R. G. Egdell, D. S. L. Law, A. Vittadini, M. Casarin, Phys. Rev. B. 61, 13445 (2000).

[50] T. J. Coutts, D. L.Young, and X. Li, MRS bulletin 25, 58 (2000).

[51] T. Koida and M. Kondo, Appl. Phys. Lett. 89, 082104 (2006).